

Crystal Dynamics of Sodium at 90°K

A. D. B. WOODS, B. N. BROCKHOUSE,* R. H. MARCH,** AND A. T. STEWART†
Neutron Physics Branch, Atomic Energy of Canada Limited, Chalk River, Ontario, Canada

AND

R. BOWERS‡
Laboratory of Atomic and Solid State Physics, Cornell University, Ithaca, New York

(Received June 4, 1962)

The frequency/wave vector dispersion relations for the lattice vibrations of sodium have been measured by neutron spectrometry along the symmetric lines $[00\zeta]$, $[\zeta\zeta0]$, $[\zeta\zeta\zeta]$, $[\frac{1}{2}\frac{1}{2}\zeta]$, and $[\zeta\zeta1]$ and at several nonsymmetric points in the reduced zone. The measurements were made at 90°K using the triple-axis crystal spectrometer in the constant \mathbf{Q} mode of operation. The results can be qualitatively described by a first- and second-neighbor force model but detailed analysis shows that fourth- and fifth-neighbor forces are probably significant. The calculated force constants for fifth neighbors are about 1 or 2% of those for first neighbors. Discontinuities in the slopes of the dispersion curves due to the Fermi surface (the Kohn effect) were not observed.

I. INTRODUCTION

AS part of the program for investigating the properties of lattice waves and interatomic forces in metals a detailed study has been made of the frequency wave vector dispersion relations in sodium. A similar study of lead was described in the preceding paper.¹ Many of the experimental details and other pertinent considerations were discussed in detail there and need only be described briefly in this paper. Preliminary results on the dispersion relations in the symmetry directions in sodium have already been published² but no quantitative conclusions concerning the interatomic force constants were reached.

The relationship between the Born-von Kármán theory of lattice dynamics³ and the scattering of slow neutrons⁴ is discussed in the preceding paper.¹ The changes in wavelength of the scattered neutrons lead directly to the dispersion relations between the frequencies and wave vectors of normal modes of vibration of the crystal.

The present paper is concerned mainly with the experimental determination of the dispersion relations for the lattice vibrations in sodium at 90°K and the analysis of these results to obtain interatomic force constants. The analysis shows that long-range interactions between the metallic ions are important although not so important as in lead.¹ An attempt was also made to determine the polarizations of some off-

symmetry modes from intensity measurements. Measurements were also made at 215 and 296°K. The frequencies were, in general, a few percent lower at the higher temperatures than at 90°K. The widths of the neutron groups increased with increased temperature suggesting, as in the case of lead, that at temperatures approaching the melting point phonon lifetimes in sodium are very short. This aspect of the experiments will be discussed in more detail in a separate paper.

II. THEORY OF THE LATTICE DYNAMICS OF SODIUM

1. Previous Work

The lattice dynamics for a body-centered cubic crystal, and in particular for sodium, have been discussed extensively in the literature. Fine⁵ and Bauer⁶ made calculations in which they took into account central forces between first and second neighbors. Fine applied his calculations to tungsten, Bauer to sodium. Bhatia⁷ used a model for sodium which took account of the direct influence of the conduction electrons but in such a way that they affected only the longitudinal vibrations. Thus, his dispersion curves were not periodic in the reciprocal lattice, a condition which is required by symmetry.

More recently, Toya⁸ has calculated the dispersion curves for the lattice vibrations of sodium in a more fundamental way. The agreement between his calculations and the experimental results has already been shown to be quite good.²

2. Born-von Kármán Theory

In this section the Born-von Kármán theory for a body-centered cubic lattice with interactions out to fifth neighbors will be considered. In the harmonic

* Now at Department of Physics, McMaster University, Hamilton, Ontario, Canada.

** Summer visitor (1960) now at Clarendon Laboratory, Oxford, England.

† Summer visitor (1961) from University of North Carolina, Chapel Hill, North Carolina.

‡ Supported in part by U. S. Atomic Energy Commission.
¹ B. N. Brockhouse, T. Arase, G. Caglioti, K. R. Rao, and A. D. B. Woods, preceding paper [Phys. Rev. **128**, 1099 (1962)].

² A. D. B. Woods, B. N. Brockhouse, R. H. March, and R. Bowers, Proc. Phys. Soc. (London) **79**, 440 (1962) and Bull. Am. Phys. Soc. **6**, 261 (1961).

³ M. Born and K. Huang, *Dynamical Theory of Crystal Lattices* (Oxford University Press, New York, 1954).

⁴ R. Weinstock, Phys. Rev. **65**, 1 (1944).

⁵ P. C. Fine, Phys. Rev. **56**, 355 (1939).

⁶ E. Bauer, Phys. Rev. **92**, 58 (1953).

⁷ A. B. Bhatia, Phys. Rev. **97**, 363 (1955).

⁸ T. Toya, J. Research Inst. Catalysis, Hokkaido Univ. **6**, 183 (1958).

approximation the equation of motion for a system with one atom per unit cell is

$$M\ddot{u}_\alpha(l) = \sum_\beta \sum_{l'} \Phi_{\alpha\beta}(ll') u_\beta(l'), \quad (1)$$

where M is the mass of the atom, u is the displacement from equilibrium, l indicates the cell position, α, β are directions in the crystal, and $\Phi_{\alpha\beta}(l, l')$ is the force in the α direction on the atom in the l th cell when the atom in cell l' is moved unit distance in the β direction. This is called the force constant. The solution of the equation can be written in terms of plane waves of frequency ν and wave vector \mathbf{q} . These are the normal modes of vibration. This solution leads to the set of equations

$$4\pi^2\nu^2(\mathbf{q})M\xi_\alpha(\mathbf{q}) = \sum_\beta C_{\alpha\beta}(\mathbf{q})\xi_\beta(\mathbf{q}), \quad (2)$$

where ξ_α, ξ_β are components of the polarization vector ξ of the mode and

$$C_{\alpha\beta}(\mathbf{q}) = \sum_{l'} \Phi_{\alpha\beta}(l, l') \exp\{i\mathbf{q} \cdot [\mathbf{R}(l) - \mathbf{R}(l')]\} \\ = -\sum_{l'} \Phi_{\alpha\beta}(l, l') \{1 - \cos[\mathbf{q} \cdot \mathbf{R}(l')]\}, \quad (3)$$

where the l th unit cell has been taken as the origin and the summation is over values of $l' \neq 0$. The imaginary

terms sum to zero because of the crystal symmetry. The frequencies of the normal modes of vibration are given by solutions of the determinantal equation

$$|4\pi^2\nu^2(\mathbf{q})M\delta_{\alpha\beta} - C_{\alpha\beta}(\mathbf{q})| = 0. \quad (4)$$

Under special conditions this 3×3 determinant reduces to a set of linear equations. For a body-centered cubic crystal this occurs for

1. Waves propagating in the three directions of highest symmetry: $[00\zeta]$, $[\zeta\zeta 0]$, and $[\zeta\zeta\zeta]$. In these cases the determinant factors into three linear equations.

2. Waves with the terminus of \mathbf{q} lying on the lines $[\frac{1}{2}\frac{1}{2}\zeta]$ and $[\zeta\zeta 1]$. These waves are neither longitudinal nor transverse but their polarization vectors are completely determined from symmetry.

3. Waves propagating in a mirror plane. In this case two of the polarization vectors are in the mirror plane and the third is perpendicular to it. Correspondingly, the 3×3 determinant becomes a product of a linear equation (in ν^2) and a 2×2 determinant. This 2×2 determinant becomes a linear equation in the sum of

TABLE I. Interatomic force constant composition of interplanar force constants Φ_n for symmetry branches in a body-centered cubic crystal.

Position of atom \rightarrow			$\frac{1}{2}a(1,1,1)$		$\frac{1}{2}a(2,0,0)$		$\frac{1}{2}a(2,2,0)$			$\frac{1}{2}a(3,1,1)$			$\frac{1}{2}a(2,2,2)$		
Branch	ζ_{\max}	n	α_1 $\langle x, x \rangle$	β_1 $\langle x, y \rangle$	α_2 $\langle x, x \rangle$	β_2 $\langle y, y \rangle$	α_3 $\langle x, x \rangle$	β_3 $\langle z, z \rangle$	γ_3 $\langle x, y \rangle$	α_4 $\langle x, x \rangle$	β_4 $\langle y, y \rangle$	γ_4 $\langle y, z \rangle$	δ_4 $\langle x, y \rangle$	α_5 $\langle x, x \rangle$	β_5 $\langle x, y \rangle$
$[00\zeta] L$	1	1 2 3	8		2		8				16			8	
$[00\zeta] T$	1	1 2 3	8			2	4	4		8	8				
$[\zeta\zeta 0] L$	0.5	1 2	4	4	2	2	4	4	2	4	8	4	-8	4	4
$[\zeta\zeta 0] T_1$	0.5	1 2	4	-4	2	2	4	4	-2	4	8	-4	8	4	-4
$[\zeta\zeta 0] T_2$	0.5	1 2	4			4	8			4	8		-8	4	
$[\zeta\zeta\zeta] L$	1	1 2 3 4 5 6	6	-4	2	4		2		2	4	4	-8	6	-4
$[\zeta\zeta\zeta] T$	1	1 2 3 4 5 6	6	2	2	4				2	4	-2	4	6	2
$[\frac{1}{2}\frac{1}{2}\zeta] \Lambda$	1	0 2	8		2	8	16	-8		8	16			8	
$[\frac{1}{2}\frac{1}{2}\zeta] \Pi$	1	0 1 2 3	8	8	4	4	8	8		8	16	8	-16	8	
$[\zeta\zeta 1] \Pi_1$	0.5	0 1 2	16	-4	2	2	4	4	2	16	32	-4	8	4	4
$[\zeta\zeta 1] \Pi_2$	0.5	0 1 2	16	-4		4	8		2	16	32	-4	-8	4	

TABLE II. Interatomic force constant composition of Φ_n for the sums of squares of the frequencies for nonsymmetric branches in a (110) plane of a body-centered cubic crystal.

Position of atom →		$\frac{1}{2}a(1,1,1)$		$\frac{1}{2}a(2,0,0)$		$\frac{1}{2}a(2,2,0)$			$\frac{1}{2}a(3,1,1)$			$\frac{1}{2}a(2,2,2)$				
Branch	ζ_{\max}	n	α_1 $\langle x,x \rangle$	β_1 $\langle x,y \rangle$	α_2 $\langle x,x \rangle$	β_2 $\langle y,y \rangle$	α_3 $\langle x,x \rangle$	β_3 $\langle z,z \rangle$	γ_3 $\langle x,y \rangle$	α_4 $\langle x,x \rangle$	β_4 $\langle y,y \rangle$	γ_4 $\langle y,z \rangle$	δ_4 $\langle x,y \rangle$	α_5 $\langle x,x \rangle$	β_5 $\langle x,y \rangle$	
[$\zeta\zeta$ 2 ζ]	0.5	1	8	-4	2	6	6	2	2	2	6	2	4	8	-4	
		2	4	2	2	2	2	2	2	4	8	-4	-4	4	2	
		3						6	2		6	10	-4	4		
		4								2	2	2	2		4	2
[$\zeta\zeta$ 1-2 ζ]	0.5	0	32							32	64					
		1	-8	4	2	6	6	2		-2	-6		-4			
		2	-4	-2	2	2	2	2	2	2	-4	-8	-2	4	8	-4
		3						6	2		-6	-10	4	-4		
[$\zeta\zeta$ $\frac{1}{2}$]	0.5	0	16-8 $\sqrt{2}$		2	2	12	4		16	32-8 $\sqrt{2}$				16	
		1	4 $\sqrt{2}$	2 $\sqrt{2}$	2	6					4 $\sqrt{2}$	-2 $\sqrt{2}$	-4 $\sqrt{2}$			
		2					2	2	2	2 $\sqrt{2}$	6 $\sqrt{2}$			4 $\sqrt{2}$		
		2														
[$\zeta\zeta$ $\frac{1}{2}$]	0.5	0	16		4	4	24	8		16	32				32	
		1			2	6	-12	-4								
		2					2	2	2						-8	-4
		2														
[$\zeta\zeta$ $\frac{3}{4}$]	0.5	0	16+8 $\sqrt{2}$		2	2	12	4		16	32+8 $\sqrt{2}$				16	
		1	-4 $\sqrt{2}$	-2 $\sqrt{2}$	2	6					-4 $\sqrt{2}$	2 $\sqrt{2}$	4 $\sqrt{2}$			
		2					2	2	2	-2 $\sqrt{2}$	-6 $\sqrt{2}$			-4 $\sqrt{2}$		
		2														
[$\frac{1}{8}\frac{1}{8}\zeta$]	1	0	8-4 $\sqrt{2}$	4-2 $\sqrt{2}$	2- $\sqrt{2}$	6-3 $\sqrt{2}$	14-6 $\sqrt{2}$	6-2 $\sqrt{2}$	2	12-4 $\sqrt{2}$	28-8 $\sqrt{2}$	4-2 $\sqrt{2}$	4 $\sqrt{2}$	8	4	
		1	8+4 $\sqrt{2}$	-4+2 $\sqrt{2}$						2 $\sqrt{2}$	6 $\sqrt{2}$			-4 $\sqrt{2}$		
		2			2	2	6 $\sqrt{2}$	2 $\sqrt{2}$						8	-4	
		3								4+2 $\sqrt{2}$	4+2 $\sqrt{2}$	-4+2 $\sqrt{2}$				
[$\frac{1}{4}\frac{1}{4}\zeta$]	1	0	8	4	2	6	16	8	4	16	40	4	8	16	8	
		1	8	-4							-4	-12		-8		
		2			2	2										
		3									4	4	-4		-8	
[$\frac{3}{8}\frac{3}{8}\zeta$]	1	0	8+4 $\sqrt{2}$	4+2 $\sqrt{2}$	2+ $\sqrt{2}$	6+3 $\sqrt{2}$	14+6 $\sqrt{2}$	6+2 $\sqrt{2}$	2	12+4 $\sqrt{2}$	28+8 $\sqrt{2}$	4+2 $\sqrt{2}$	-4 $\sqrt{2}$	8	4	
		1	8-4 $\sqrt{2}$	-4-2 $\sqrt{2}$							-2 $\sqrt{2}$	-6 $\sqrt{2}$		4 $\sqrt{2}$		
		2			2	2	-6 $\sqrt{2}$	-2 $\sqrt{2}$							8	-4
		3									4-2 $\sqrt{2}$	4-2 $\sqrt{2}$	-4-2 $\sqrt{2}$			

the squares of the frequencies of the two normal modes at any given value of q .

In what follows, the elements of the force constant matrices, $\Phi_{\alpha\beta}(l')$, will be denoted by small Greek letters with subscripts to indicate the appropriate neighbor. Thus, $\alpha_1 \equiv \Phi_{11}(111)$ denotes the force on the atom at the origin in direction 1 when the nearest-neighbor atom (at position 1, 1, 1 in units of $a/2$) is moved unit distance in direction 1. Similarly, $\Phi_{12}(111) = \beta_1$, $\Phi_{11}(200) = \alpha_2$, etc.

The solution of Eq. (4) for the three cases discussed above leads to an equation in ν^2 of the form

$$4\pi^2 M \nu^2 = \sum_n \Phi_n (1 - \cos n\pi\zeta/\zeta_{\max}),$$

where Φ_n is a linear combination of the force constants $\alpha_1, \beta_1, \alpha_2$, etc., the coefficients of these force constants being a function of the particular direction and branch which is under consideration. Table I summarizes completely the lattice dynamics in the symmetric directions for a body-centered cubic crystal on the assumption of harmonic restoring forces out to fifth neighbors. The extension to the sums of the squares of the frequencies of the two modes vibrating in the (110) mirror plane is given in Table II. The determination of the interplanar force constants, Φ_n , and the interatomic force constants, α_n , etc., from the experimental dispersion curves is discussed in Sec. V.

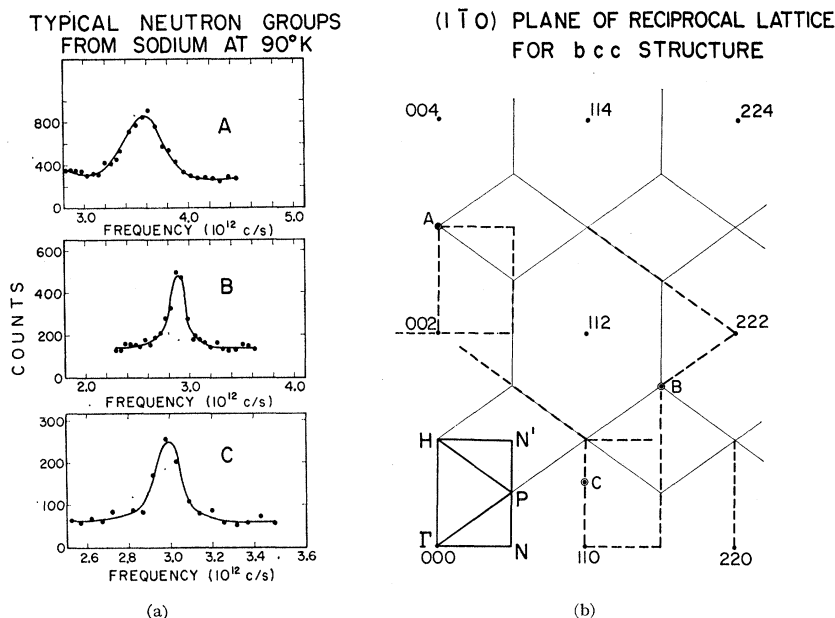
III. SPECIMEN PREPARATION

Single crystals of sodium,⁹ approximately 2 in. in diameter and 4 in. long, were grown by a modification of the Bridgman method due to Daniels.¹⁰ This method uses a stationary vertical tube of stainless steel on which is wound a heating coil with a variable spacing such that the top of the tube is heated more than the bottom. The bottom of the tube is closed by a stainless steel plug to which is attached a coil of copper tubing through which air is passed for cooling. Sodium is melted in the tube under mineral oil and by control of the heating and cooling it is possible to solidify the sodium in a directional manner, the solid interface moving from the bottom to the top. With cooling times of 1 or 2 h, most of the resulting boules were single crystals. The crystals were etched in xylene containing one part in 50 of isopropyl alcohol; preliminary cleaning was done in methyl and isopropyl alcohol. The sodium

⁹ Our techniques for growing, cutting, and etching single crystals of sodium have been described in detail in a report: "Single Crystals of Sodium and Lithium," by R. Bowers, D. Pinnow, and S. Tallman, Report No. 3, Materials Science Center, Cornell University (unpublished). Copies of this report can be obtained from the Materials Science Center, Cornell University, Ithaca, New York. In view of the availability of this report, our description of crystal-growing techniques in the present paper will be limited to a brief outline.

¹⁰ W. B. Daniels, Phys. Rev. **119**, 1246 (1960).

Fig. 1(a) Typical neutron distributions plotted as a function of frequency. Curves *A* and *B* have a fast neutron background, ~ 150 counts per point, subtracted. The fast neutron background for Curve *C*, ~ 30 counts per point, has not been subtracted. (b) The $(1\bar{1}0)$ plane of the reciprocal lattice for a bcc structure. The points marked *A*, *B*, and *C* indicate, respectively, the \mathbf{Q} positions for the neutron groups marked *A*, *B*, and *C* on the left-hand side. The light solid lines indicate zone boundaries. The heavy dashed lines show the lines in the reciprocal lattice on which most of the measurements were made. The rectangle $\Gamma NP'N'H\Gamma$ is the irreducible zone which contains all frequencies observable in this plane. The line $\Gamma H \equiv [00\bar{\zeta}]$, $\Gamma N \equiv [\zeta\zeta 0]$, $\Gamma P H \equiv [\zeta\zeta\zeta]$, $H N' \equiv [\zeta\zeta 1]$, and $N N' \equiv [\frac{1}{2}\frac{1}{2}\zeta]$.



used for the neutron work was Mallinckrodt analytical grade material for the specimen with its $(1\bar{1}0)$ plane horizontal and Dupont reactor grade material for the specimen which had its (001) plane horizontal (see Sec. IV). These materials have a chemical purity exceeding 99.99%. Their residual resistance ratios ($\rho_{300^\circ\text{K}}/\rho_{4^\circ\text{K}}$) are approximately 1000 in each case.

Sections of length $1\frac{3}{4}$ in. were cut from the single-crystal boules using a string saw of cotton thread charged with a 50% methanol-50% water mixture. The ends and sides were lapped smooth using a cotton cloth charged with methanol. The resulting smooth cylindrical specimen was sealed in a thin-walled aluminum can whose dimensions were only slightly larger than the crystal. The cylindrical side and flat top of this can had been spun to the correct shape from a single sheet of 10-mil aluminum and hence there were no soldered joints. A much thicker aluminum base was fitted into the bottom of this cylinder. The base was equipped with side arms for attaching the specimen to the spectrometer crystal holder. The cylindrical sodium crystal, finally having a length and diameter of about $1\frac{3}{4}$ in., was cleaned with alcohol, placed without delay inside the close fitting thin-walled aluminum cylinder and the base was sealed in an airtight manner onto this cylinder by means of glue. There is probably a thin superficial layer of hydroxide on the sodium crystal but this is not expected to be detectable in the neutron data. No further contamination of the specimen is expected inside the sealed can. The form of the final specimen is such that for a wide range of directions, the neutron beam passes through approximately 2 in. of sodium and two 10-mil walls of aluminum, the scattering due to the latter being inconsequential.

IV. EXPERIMENTS AND RESULTS

1. Dispersion Curves at 90°K

The specimen was mounted inside an aluminum radiation shield, placed in a large vacuum chamber, and cooled from above with liquid nitrogen. The temperature was measured with a copper constantan thermocouple and was continuously recorded. For most of the experiments the crystal was mounted so that its $(1\bar{1}0)$ plane was horizontal. Less extensive measurements were made with a (001) plane horizontal.

The experiment consisted in measuring the energy distributions of neutrons scattered from the specimen. This was done using the triple axis crystal spectrometer in the "constant \mathbf{Q} " mode¹¹ of operation. Neutron energy loss and variable input energy were used exclusively. Several typical distributions are shown in Fig. 1(a) as a function of the frequency of the phonon excited in the crystal. The $(1\bar{1}0)$ plane of the reciprocal lattice is shown in Fig. 1(b) and the positions of the three neutron groups in Fig. 1(a) are indicated by the letters *A*, *B*, and *C*. Most of the experiments were carried out along the heavy dashed lines in Fig. 1(b).

Measurements were made at 90°K for \mathbf{q} on the symmetric lines $[00\bar{\zeta}]$, $[\zeta\zeta 0]$, $[\zeta\zeta\zeta]$, $[\frac{1}{2}\frac{1}{2}\zeta]$, and $[\zeta\zeta 1]$ and for several values of \mathbf{q} in nonsymmetry directions. Table III lists the observed phonons and the results for the symmetric directions at 90°K are shown in Fig. 2.

It is interesting to observe how the various symmetry properties of the bcc structure are illustrated by these results. At the zone boundary for the $[00\bar{\zeta}]$ direction

¹¹ For a detailed discussion of this method, see B. N. Brockhouse, *Inelastic Scattering of Neutrons in Solids and Liquids* (International Atomic Energy Agency, Vienna, 1961), p. 113.

TABLE III. Frequencies (units 10^{12} cps) of normal modes on symmetric branches in sodium at 90°K . The modes marked with an asterisk are included on more than one branch.

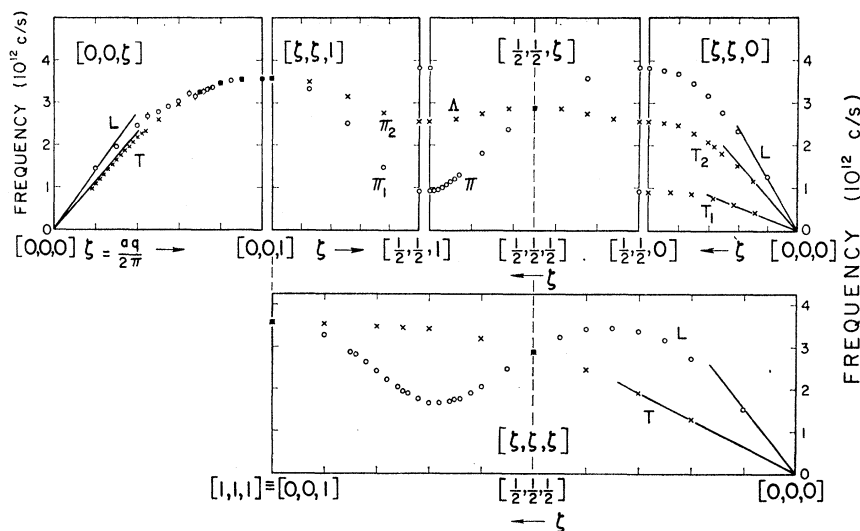
$\zeta = aq/2\pi$	ν	$\zeta = (1/\sqrt{2})(aq/2\pi)$	ν	$\zeta = (1/\sqrt{3})(aq/2\pi)$	ν	ζ	ν
	$[00\zeta] L$		$[\zeta\zeta 0] L$		$[\zeta\zeta\zeta] L$		$[\frac{1}{2} \frac{1}{2} \zeta] A$
0.20	1.43±0.07	0.10	1.25±0.04	0.10	1.53±0.05	0*	2.56±0.05
0.30	1.94±0.06	0.20	2.32±0.03	0.20	2.72±0.06	0.125	2.62±0.06
0.40	2.44±0.05	0.25	2.77±0.05	0.25	3.16±0.06	0.25	2.74±0.06
0.45	2.68±0.1	0.30	3.17±0.05	0.30	3.38±0.06	0.375	2.92±0.07
0.50	2.78±0.06	0.35	3.46±0.06	0.35	3.44±0.05	0.50*	2.88±0.04
0.55	2.91±0.07	0.40	3.67±0.05	0.40	3.42±0.06	0.625	2.80±0.08
0.60	3.01±0.07	0.45	3.75±0.09	0.45	3.22±0.06	0.75	2.73±0.07
0.65	3.19±0.07	0.50*	3.82±0.07	0.50*	2.88±0.04	1.00*	2.56±0.05
0.68	3.14±0.1			0.55	2.48±0.05		
0.70	3.24±0.06		$[\zeta\zeta 0] T_1$	0.60	2.06±0.04		$[\frac{1}{2} \frac{1}{2} \zeta] II$
0.72	3.25±0.08			0.62	1.90±0.04		
0.74	3.31±0.08	0.14	0.43±0.03	0.64	1.78±0.04	0*	3.82±0.07
0.75	3.36±0.1	0.21	0.61±0.03	0.65	1.74±0.03	0.25	3.57±0.08
0.76	3.36±0.07	0.28	0.76±0.03	0.66	1.71±0.04	0.50*	2.88±0.04
0.80	3.44±0.05	0.35	0.87±0.03	0.68	1.67±0.04	0.625	2.38±0.06
0.85	3.53±0.06	0.42	0.92±0.04	0.70	1.68±0.03	0.75	1.81±0.05
0.90	3.55±0.05	0.50*	0.93±0.02	0.72	1.78±0.05	0.86	1.28±0.04
1.00*	3.58±0.04			0.725	1.77±0.05	0.88	1.23±0.04
			$[\zeta\zeta 0] T_2$	0.74	1.89±0.05	0.90	1.14±0.03
	$[00\zeta] T$	0.15	1.16±0.04	0.75	1.94±0.04	0.92	1.07±0.03
0.18	0.97±0.03	0.20	1.52±0.04	0.76	2.04±0.04	0.94	1.01±0.03
0.20	1.09±0.04	0.25	1.81±0.03	0.78	2.22±0.05	0.96	0.96±0.04
0.22	1.18±0.04	0.28	1.97±0.03	0.80	2.43±0.04	0.98	0.93±0.03
0.24	1.29±0.04	0.30	2.09±0.03	0.82	2.64±0.07	1.00*	0.93±0.02
0.26	1.42±0.04	0.35	2.27±0.04	0.84	2.82±0.09		
0.28	1.52±0.04	0.40	2.47±0.04	0.85	2.87±0.05		$[\zeta\zeta 1] II_1$
0.30	1.64±0.03	0.45	2.52±0.06	0.90	3.28±0.06		
0.32	1.74±0.05	0.50*	2.56±0.05	1.00*	3.58±0.04	0*	3.58±0.04
0.34	1.83±0.04					0.125	3.33±0.07
0.36	1.94±0.05				$[\zeta\zeta\zeta] T$	0.25	2.50±0.05
0.38	2.07±0.05			0.20	1.28±0.06	0.375	1.49±0.04
0.40	2.17±0.04			0.30	1.92±0.06	0.50*	0.93±0.02
0.42	2.25±0.05			0.40	2.47±0.05		
0.44	2.32±0.04			0.50*	2.88±0.04		$[\zeta\zeta 1] II_2$
0.50	2.59±0.05			0.60	3.21±0.06	0*	3.58±0.04
0.60	2.96±0.03			0.70	3.42±0.06	0.125	3.48±0.07
0.70	3.23±0.04			0.72	3.44±0.09	0.25	3.14±0.06
0.75	3.35±0.04			0.74	3.46±0.09	0.375	2.75±0.06
0.80	3.45±0.05			0.75	3.46±0.05	0.50*	2.56±0.05
0.90	3.57±0.06			0.76	3.44±0.09		
1.00*	3.58±0.04			0.78	3.44±0.09		
				0.80	3.48±0.05		
				0.82	3.48±0.09		
				0.84	3.54±0.09		
				0.86	3.52±0.09		
				0.90	3.56±0.05		
				1.00*	3.58±0.04		

[the point (0,0,1)] the longitudinal and transverse branches are degenerate by symmetry. The longitudinal and transverse modes are degenerate, also by symmetry, at the point $(\frac{1}{2}, \frac{1}{2}, \frac{1}{2})$. This is illustrated in the curves $[\zeta\zeta\zeta]$ and $[\frac{1}{2} \frac{1}{2} \zeta]$. The upper curves show the frequencies of phonons whose coordinates in the reduced zone of the reciprocal lattice on the perimeter of the rectangle $\Gamma N P N' H \Gamma$ in Fig. 1. The line $[\zeta\zeta\zeta]$ and its mirror reflection in the upper half of the reduced zone make contact with this rectangle at the points (0,0,0), $(\frac{1}{2}, \frac{1}{2}, \frac{1}{2})$ and (0,0,1). At the point $(\frac{1}{2}, \frac{1}{2}, 1)$ it is possible to determine the frequency of the zone boundary mode for the second transverse branch in the $[\zeta\zeta 0]$ direction. This point is on the zone boundary for the (1,0,1) reciprocal lattice point which is not in the $(1\bar{1}0)$ plane. By symmetry the polarizations of the two modes vibrating in

the $(1\bar{1}0)$ plane at this point are both transverse. One of these transverse modes is just the endpoint of the $[\zeta\zeta 0] T_1$ branch. The complete $[\zeta\zeta 0] T_1$ branch has been determined by using a (different) specimen which had its (001) plane horizontal. With this specimen more measurements were also made in the $[00\zeta]$ direction which verified the earlier results.

In the course of the measurements, particularly those along the $[00\zeta] L$ branch, peaks in the neutron distribution corresponding to lower energy transfer were observed. These peaks have been attributed to multiple (elastic plus inelastic) scattering¹ in the crystal. The mosaic spread of the (002) plane of the sodium crystal was about 0.14 deg, and thus such multiple scattering events are not expected to be frequent. Hence, their appearance was surprising, especially since their energy

FIG. 2. The dispersion curves for sodium at 90°K. The solid lines have been calculated from the best available values of the elastic constants at 90°K (reference 17). The abscissa for the $[\xi\xi\xi]$ direction has been stretched to emphasize the equivalence of the points $[\frac{1}{2}\frac{1}{2}\frac{1}{2}]$ and $[111]$ with the corresponding points for $[\frac{1}{2}\frac{1}{2}\xi]$ and $[00\xi]$ shown above.



did not correspond exactly with that of the transverse branch. However, in every case examined, such multiple scatterings were possible and usually involved two wave vectors out of the horizontal plane. In these cases other considerations can change the apparent value of ν for the phonon. This contaminant intensity had considerable effect only on the $[00\xi]$ L branch. For all other branches conditions were arranged so that sharp and apparently uncontaminated groups could be obtained.

2. Measurements of Polarization Vectors

Besides the measurements of the dispersion curves for vibrations in the symmetry directions in the crystal several off-symmetry modes were also measured. The frequencies of these modes are shown in Table IV. In the irreducible rectangle in Fig. 3 the approximate polarization directions are indicated by the arrow heads; the directions were inferred from continuity with the symmetry directions and from intensity observations.

The relative integrated intensities of two modes of unknown, but mutually perpendicular, polarizations were measured by plotting the neutron distributions on an energy scale and correcting for the difference in frequency between the two modes. No other corrections were necessary since the factors k'/k_0 and $1/|J|$ in

the one-phonon intensity formula¹² were automatically included.

The factor k'/k_0 was eliminated because variable input energy was used¹¹ in the experiment and the monitor counter in the diffracted beam had a $1/\nu$ sensitivity. Because of the constant Q method of making measurements the factor $1/|J|=1$ for all phonons. The chief difficulty in deducing intensities is in deciding just where to draw the background level under each peak. For sodium this background is large because of the large incoherent scattering cross section. The experiments will be discussed in more detail elsewhere.¹³

TABLE IV. Frequencies (units 10^{12} cps) of some nonsymmetric modes at 90°K.

Mode	ν_1	ν_2
$(\frac{1}{16} \frac{1}{16} \frac{1}{16})$	1.68 ± 0.05	
$(\frac{3}{16} \frac{3}{16} \frac{1}{16})$	2.50 ± 0.05	0.93 ± 0.03
$(\frac{5}{16} \frac{5}{16} \frac{1}{16})$	3.32 ± 0.07	1.88 ± 0.04
$(\frac{7}{16} \frac{7}{16} \frac{1}{16})$	3.59 ± 0.06	2.76 ± 0.05
$(\frac{9}{16} \frac{9}{16} \frac{1}{16})$	3.56 ± 0.05	1.54 ± 0.04
$(\frac{11}{16} \frac{11}{16} \frac{1}{16})$	3.49 ± 0.05	2.43 ± 0.05
$(\frac{13}{16} \frac{13}{16} \frac{1}{16})$	3.36 ± 0.05	2.12 ± 0.05
$(\frac{15}{16} \frac{15}{16} \frac{1}{16})$	3.04 ± 0.06	1.64 ± 0.05
$(\frac{7}{16} \frac{7}{16} \frac{1}{8})$	3.65 ± 0.06	

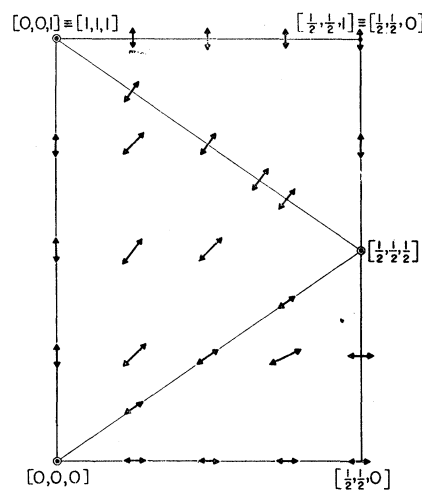


FIG. 3. The approximate polarization directions for the high-frequency mode in the (110) plane. These were deduced from symmetry considerations, intensity measurements, dispersion curve continuity, and the values of the force constants for the fifth neighbor model.

¹² I. Waller and P. O. Froman, Arkiv Fysik 4, 183 (1952).

¹³ B. N. Brockhouse, L. N. Becka, K. R. Rao, and A. D. B. Woods, I.A.E.A. Symposium on Inelastic Scattering of Neutrons in Solids and Liquids, Chalk River, Ont., Sept. 10-14, 1962. Also issued as Chalk River Report, AECL-1572.

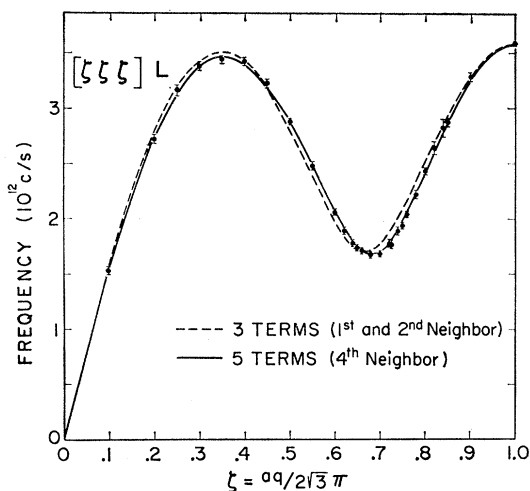


FIG. 4. Fourier series fits to the $[\zeta\zeta\zeta] L$ branch of sodium. A three-term fit is not quite adequate quantitatively although it represents a good qualitative description.

3. Search for Kohn Effect

Kohn¹⁴ has predicted that there will be a kink in the dispersion curves for a metal when the wave vector, \mathbf{q} , of the phonon plus any reciprocal lattice vector ($2\pi\boldsymbol{\tau}$) is equal to the diameter (in the spherical case) of the Fermi surface. Such effects have been observed in lead¹⁵ and are discussed in detail in the preceding paper.¹ Considerable effort was spent to see if the effect could be observed in sodium at 90°K. Four regions of reciprocal space were investigated which corresponded to a free electron spherical Fermi surface of radius 0.146 \AA^{-1} . The range of q studied allowed for a variation of $\pm 5\%$ in the Fermi radius. The branches studied were $[00\zeta] T$ near $\zeta=0.3$, $[00\zeta] L$ near $\zeta=0.75$, $[\frac{1}{2}\frac{1}{2}\zeta] \pi$ near $\zeta=1$, and $[\zeta\zeta\zeta] L$ near $\zeta=0.7$. The measured points are included in Figs. 2 and 4 and show no evidence of any anomaly within an accuracy $\sim 1\%$. The only case of doubt is the $[00\zeta] L$ branch where, as explained earlier, it was not possible to obtain sharp uncontaminated neutron groups. The close proximity (in frequency) of the transverse branch probably complicates the situation still further.

Thus, we have no evidence for the existence of well-marked Kohn anomalies in sodium; nor are they expected¹ to be large since, compared with lead, the electron-phonon interaction is very small.

V. ANALYSIS OF EXPERIMENTAL RESULTS

1. Fourier Analysis

In the Born-von Kármán theory, the coefficients of the sinusoidal terms in the expressions for ν^2 in

¹⁴ W. Kohn, Phys. Rev. Letters **2**, 393 (1959).

¹⁵ B. N. Brockhouse, K. R. Rao, and A. D. B. Woods, Phys. Rev. Letters **7**, 530 (1961).

TABLE V. Interplanar force constants Φ_n for sodium at 90°K in units of 10^9 dyn/cm . Only those contributed to by five neighbors are included. The errors shown are those incurred in fitting. Absolute errors are somewhat larger.

	Φ_0	Φ_1	Φ_2	Φ_3	Φ_4	Φ_5	Φ_6	error
$[00\zeta] L$...	93.6	8.7	3.4				± 0.6
$[00\zeta] T$...	98.2	2.1	-1.1				± 0.3
$[\zeta\zeta 0] L$...	110.7	3.1					± 0.5
$[\zeta\zeta 0] T_1$...	6.7	0.1					± 0.1
$[\zeta\zeta 0] T_2$...	49.8	-0.03					± 0.4
$[\zeta\zeta\zeta] L$...	17.5	13.4	77.8	-4.3	1.7	0.8	± 0.4
$[\zeta\zeta\zeta] T$...	97.5	15.3	-1.6	-0.2	1.1	-1.3	± 0.7
$[\frac{1}{2}\frac{1}{2}\zeta] A$	99.1	...	13.6	...				± 1.5
$[\frac{1}{2}\frac{1}{2}\zeta] B$	220.2	-102.4	4.2	-1.2				± 0.4
$[\zeta\zeta 1] \Pi_1$	194.1	-91.0	-3.8					± 2.0
$[\zeta\zeta 1] \Pi_2$	194.0	-47.7	1.3					± 1.0

symmetry directions are linear combinations of the force constants between atoms (see Table II). Furthermore, it has been shown that these linear combinations of interatomic force constants are just the force constants between corresponding planes of atoms. Thus, a Fourier series analysis^{1,16} for the squares of the measured frequencies on the dispersion curves will yield the interplanar force constants; the number of terms in the Fourier series required to fit the data gives the range of the interplanar force constants and hence the minimum range for the interatomic force constants. Accordingly, a least-squares Fourier fit of the form,

$$4\pi^2 M \nu^2 = \sum_{n=1}^N \Phi_n (1 - \cos n\pi\zeta/\zeta_{\max}),$$

was made for different values of n up to $N=12$ in some cases. Each phonon used in the fit was assigned a weight depending on its estimated error. The best values of the elastic constants available¹⁷ were also included in the fit with a variety of weights. The values of the interplanar force constants for interactions out to fifth neighbors are listed in Table V. As in the case of lead, it was found that the weight attached to the elastic constants had little effect upon the calculated values of the interplanar force constants. This fact attested to the consistency of the neutron data with the elastic constants.

The results of such fits to the data for the $[\zeta\zeta\zeta] L$ branch are shown in Fig. 4. For this branch, three terms

¹⁶ A. J. E. Foreman and W. M. Lomer, Proc. Phys. Soc. (London) **B70**, 1143 (1957).

¹⁷ The low-temperature elastic constants for sodium are rather poorly known. The results of O. Bender [Ann. Physik **34**, 359 (1939)], as quoted by J. de Launay, in *Solid-State Physics* [edited by F. Seitz and D. Turnbull (Academic Press Inc., New York, 1956), Vol. 2] are in serious disagreement with those of S. L. Quimby and S. Siegel [Phys. Rev. **54**, 293 (1938)]. The recent results of Daniels (reference 10) at room temperature support the values given for the shear constants by Quimby and Siegel but not their value for c_{11} . Thus for the shear constants the values given by Quimby and Siegel were used. Following the suggestion of C. S. Smith (private communication) the value used for c_{11} was a composite one, combining Daniels' room temperature value with the temperature variation given by Quimby and Siegel.

in the series are almost but not quite adequate to fit the data. This means (see Table I) that first- and second-neighbor interaction, even assuming general forces, are insufficient; the necessity for five terms in the fit implies at least fourth-neighbor interaction, if we are to remain within the framework of the Born-von Kármán theory. Similar fits have been obtained for the other branches at 90°K and support the conclusion that a force model which includes only first- and second-neighbor central forces is quite inadequate quantitatively; qualitatively, however, a first- and second-neighbor central force model does appear to give a reasonable description of the dispersion relations.

The sums of the squares of the frequencies of the two nonsymmetric modes at a given \mathbf{q} in a mirror plane can be considered in much the same way as the individual modes in the symmetric directions as discussed in Sec. II. Hence, these data can be used, in conjunction with those in the symmetric directions, for force constant analysis.

2. Interatomic Force Constants

The values of Φ_n , determined from Fourier analysis of the dispersion curves, are linear combinations of the interatomic force constants. A least-squares fit for the force constants out to fifth neighbors was performed on the Chalk River datatron; the "best" values are given in Table VI together with an estimated "error". The error given has been deduced partly from the calculated error in the fits and partly by the spread in force constant values which result when the values of Φ_n for different groups of dispersion curves are used. The amount of information contained in the measured dispersion curves is more than sufficient to permit the determination of unique values of the force constants out to fifth neighbors. The sums of squares of the frequencies at off-symmetry points were also included in some of the fits. They were not used in the final force constant determination but, instead, the individual nonsymmetric modes were used as a check on the calculated force constants.

Least-squares fits were also carried out under the assumption of central forces between the ions. This assumption leads to the following relations between the force constants:

1. The equilibrium condition³ for the crystal,

$$\alpha_1 - \beta_1 + \beta_2 + 4\beta_3 + 11\beta_4 - 11\gamma_4 + 4\alpha_5 - 4\beta_5 = 0,$$

TABLE VI. Force constants (units dynes/cm) calculated from observed frequencies. Estimated probable error is ± 10 except where indicated.

Force constant	α_1 $\langle x,x \rangle$	β_1 $\langle x,y \rangle$	α_2 $\langle x,x \rangle$	β_2 $\langle y,y \rangle$	α_3 $\langle x,x \rangle$	β_3 $\langle z,z \rangle$	γ_3 $\langle x,y \rangle$	α_4 $\langle x,x \rangle$	β_4 $\langle y,y \rangle$	γ_4 $\langle y,z \rangle$	δ_4 $\langle x,y \rangle$	α_5 $\langle x,x \rangle$	β_5 $\langle x,y \rangle$
General forces	1178	1320	472 \pm 30	104 \pm 30	-38	-0.4 \pm 30	-65	52 \pm 20	-7	3	14	17	33
Central forces	1173	1319	431 \pm 20	119 \pm 20	-47	20	-67	44	0.5	5	16	17	17

and

2. The conditions when more than two force constants per atom are involved,

$$\begin{aligned}\alpha_3 - \beta_3 - \gamma_3 &= 0, \\ \delta_4 - 3\gamma_4 &= 0, \\ \alpha_4 - \beta_4 - 8\gamma_4 &= 0.\end{aligned}$$

With these auxiliary conditions the fits were very nearly as "good" and the values of most of the calculated force constants did not change significantly. The values of α_2 , β_2 , and β_3 showed changes which were probably rather more than expected; ~ 30 dyn/cm in each case. This change may reflect the poorness of the data in some regions, e.g., $[00\xi]L$ or it may be a real measure of the departure from central forces. (It is known that the forces cannot be truly central as the elastic constants fail to satisfy the Cauchy relation; the values of c_{12} and c_{44} differ by about 15% at this temperature.¹⁷)

The qualitative features of the behavior of the force constants are the same whether or not the central force model is used. The force constants for fifth neighbors are about 1 or 2% of those for first neighbors. It is difficult to tell if the values for the fifth-neighbor force constants are really significantly different from zero; but all fits indicate that they are. If this is the case it is probably worthwhile to extend the analysis beyond fifth neighbors; the ring of eighth neighbors is the next logical stopping place. Sufficient information appears to exist to make this analysis possible but it has not been done at the present time.

VI. CONCLUSIONS

The measurements of the dispersion curves for the lattice vibrations in sodium at 90°K lead to several interesting qualitative and quantitative conclusions:

1. In contrast with lead, the results appear to be describable by the Born-von Kármán theory which requires long-range forces only to fit the finer details of the curves. First- and second-neighbor central forces give a good qualitative description; this is true of no other substance studied so far.
2. There are no apparent Kohn anomalies in the dispersion curves; they were looked for specifically at certain places at which they would be expected for a spherical Fermi surface.
3. Off-symmetry modes appear to be nearly longitudinal or transverse except near zone boundaries.

4. Although a short-range model gives an adequate qualitative picture, there is little doubt that forces out to fourth or fifth neighbors and possibly beyond, play a significant role in the determining of the details of the lattice dynamics of sodium.

5. There are still several aspects of the problem to be considered: (i) the abnormal behavior of the $[00\zeta] L$ branch, (ii) extension of the analysis to more distant neighbors, (iii) the possibility of deriving an inter-

atomic potential, and (iv) the temperature behavior of the phonons.

ACKNOWLEDGMENTS

The authors are indebted to Dr. J. M. Kennedy and Mrs. P. M. Attree for providing the computer programs for the least-squares fits, to E. A. Glaser and A. L. Bell for valuable technical assistance, and to D. Pinnow and S. Tallman for important assistance in the specimen preparation.

Lattice Vibrations in Pyrolytic Graphite

G. DOLLING AND B. N. BROCKHOUSE*

Neutron Physics Branch, Atomic Energy of Canada Limited, Chalk River, Ontario, Canada

(Received June 18, 1962)

The dispersion relation for the longitudinal acoustic lattice waves propagating in the direction of the hexad axis in (pyrolytic) graphite, at room temperature, has been determined by neutron spectrometry. The dispersion curve has very closely the form of a sine curve, with a maximum frequency of $(3.84 \pm 0.06) \times 10^{12}$ cps, for the zone-boundary phonon of wavelength $c = 6.70 \text{ \AA}$. The transverse acoustic lattice waves were less well determined, but show roughly similar behavior with a maximum frequency at the zone boundary of $(1.3 \pm 0.3) \times 10^{12}$ cps. Values for certain elastic constants have been deduced from the measurements: in units of 10^{11} dyn/cm^2 , $C_{33} = 3.9 \pm 0.4$, and $C_{44} = 0.42 \pm 0.2$.

INTRODUCTION

THE lattice dynamics of graphite has been discussed theoretically by a number of authors.¹⁻⁹ The consensus of these discussions is that the lattice modes can be approximately divided into vibrations (a) with atomic motions in the hexagonal planes of atoms and (b) with motions normal to the planes. Because the binding of the planes to each other is very much weaker than the binding of the atoms in the planes, motions of the planes with respect to one another have little influence upon the frequencies except for those relatively few modes in which the planes move substantially as rigid units. Thus, only at very low temperatures does the specific heat of graphite⁸⁻¹¹ have the familiar T^3

dependence; at intermediate temperatures it tends to display the T^2 dependence characteristic of a plane lattice. The transition between these two types of behavior is determined by the modes for which the hexagonal planes move as units; in this paper we present an experimental study of the dispersion relation for these modes at room temperature, by neutron spectrometry.

The dispersion relation between the frequency (ν) and the wave vector (\mathbf{q}) for the normal modes of vibration of a crystal lattice may be obtained by a study of the coherent one-phonon scattering of slow neutrons from a single-crystal specimen.¹² These scattering processes are governed by equations expressing conservation of energy and "crystal momentum":

$$E_0 - E' = \pm h\nu, \quad (1a)$$

$$\mathbf{Q} = \mathbf{k}_0 - \mathbf{k}' = 2\pi\boldsymbol{\tau} - \mathbf{q}, \quad (1b)$$

where E_0 , E' are the energies, and \mathbf{k}_0 , \mathbf{k}' the wave vectors, of the incident and scattered neutrons, respectively; \mathbf{Q} is the momentum transfer vector, $\boldsymbol{\tau}$ is a reciprocal lattice vector, and h is Planck's constant.

The study of the lattice vibrations of graphite by means of slow neutron scattering has so far been prevented by the lack of sufficiently large single-crystal specimens. Recently, however, the production has been

* Present address: Physics Department, McMaster University, Hamilton, Ontario, Canada.

¹ K. Komatsu and T. Nagamiya, *J. Phys. Soc. Japan* **6**, 438 (1951).

² J. A. Krumhansl and H. Brooks, *J. Chem. Phys.* **21**, 1663 (1953).

³ T. Nagamiya and K. Komatsu, *J. Chem. Phys.* **22**, 1457 (1954).

⁴ K. Komatsu, *J. Phys. Soc. Japan* **10**, 346 (1955).

⁵ G. F. Newell, *J. Chem. Phys.* **23**, 2431 (1955).

⁶ A. Yoshimori and Y. Kitano, *J. Phys. Soc. Japan* **11**, 352 (1956).

⁷ G. R. Baldock, *Phil. Mag.* **1**, 789 (1956).

⁸ J. C. Bowman and J. A. Krumhansl, *J. Phys. Chem. Solids* **6**, 367 (1958).

⁹ K. Komatsu, *J. Phys. Chem. Solids* **6**, 380 (1958).

¹⁰ W. De Sorbo and W. W. Tyler, *J. Chem. Phys.* **21**, 1660 (1953).

¹¹ W. De Sorbo and G. E. Nichols, *J. Phys. Chem. Solids* **6**, 352 (1958).

¹² See B. N. Brockhouse and A. T. Stewart, *Revs. Modern Phys.* **30**, 236 (1958).